

Search for Cascade-like events in the AMANDA-B10 detector

I. Taboada¹, M. Kowalski², and the AMANDA Collaboration³

¹Physics and Astronomy Dept. University of Pennsylvania, Philadelphia, PA 19104-6396. USA

²DESY Zeuthen, Platanenallee 6, D-15738 Zeuthen, Germany

³Complete author list is found at the end of this volume

Abstract.

The signature for the reaction of high energy ν_e ($\bar{\nu}_e$) in the AMANDA detector are isolated cascades. Compared to ν_μ -induced muons, energy resolution for ν -induced cascades is better. Also, when searching for extraterrestrial high energy neutrinos, the background from atmospheric neutrinos is lower. Data taken in 1997 with the AMANDA-B10 detector were searched for events with a cascade-like signature. The observed events are consistent with expected background from atmospheric neutrinos and catastrophic energy losses from atmospheric muons. A limit is set on the diffuse flux of $\nu_e + \bar{\nu}_e$ assuming an E^{-2} source spectrum.

1 Introduction and Motivation

While the detection of high energy atmospheric neutrinos by AMANDA has already been demonstrated via the observation of upward going muons (Andrés *et al.*, 2001), the measurement of ν -induced cascades has not been achieved yet. Demonstrating ν -induced cascade sensitivity will be an important step in neutrino astronomy, because energy resolution for cascades is better than for ν -induced muons. All ν flavors produce isolated cascades when interacting via neutral current, ν_e also produces cascades via charge current interaction. Isolated cascades may also be produced by ν_τ via charged current interaction when the energy is below ≈ 1 PeV and thus the produced τ decays after traveling a short distance from the hadronic vertex. Contributions of ν_τ to the cascade channel becomes important when flavor oscillations are taken into account for extraterrestrial and for atmospheric ν -induced cascades (Stanev, 1999).

In this work we present a search for high energy ν_e induced cascades with data taken by the AMANDA-B10 detector during the 1997 season. A limit is presented on the flux of diffuse $\nu_e + \bar{\nu}_e$ assuming an E^{-2} spectrum.

Correspondence to: I. Taboada (itaboada@hep.upenn.edu)

2 Data

As configured during 1997, AMANDA consisted of 302 optical modules, deployed on 10 strings, at depths between 1500 m and 2000 m in the Antarctic ice at the South Pole. A more complete description of the detector is available elsewhere (Hill *et al.*, 1999). The data used were collected between March and October 1997. A total of 1.45×10^9 events were recorded. The vast majority of the events recorded are muons produced in cosmic ray air showers. After correcting for dead-time (25%), the live-time of the 1997 campaign is about 130 days.

3 Monte Carlo

Monte Carlo samples have been produced for cosmic ray induced muons, atmospheric ν_e and ν_μ , and $\nu_e + \bar{\nu}_e$ with E^{-2} spectrum. Earth Absorption and neutral current neutrino regeneration are negligible effects for atmospheric neutrinos but they are taken into account for the E^{-2} spectrum Monte Carlo.

4 Methods for Cascade Reconstruction

Two algorithms are used in the present analysis to reconstruct cascades. One method reconstructs the position and time of a cascade. The other reconstruction method provides the energy and direction of a cascade. Other parameters that characterize cascades, *e.g.* length development, are not applicable with the sparsely instrumented AMANDA detector. Also AMANDA is presently unable to distinguish electromagnetic cascades from hadronic cascades.

4.1 Position and Time Reconstruction: Time Delays

This method uses a Cherenkov model that takes into account absorption and scattering of light. This procedure is quite similar to the algorithms used for muon fitting (Wiebusch,

1998). Also a more comprehensive description of the different cascade reconstruction methods can be found in (Kowalski, 1999).

The following function is a parametrization of the probability distribution of observing one photo-electron with a time delay, $t_{\text{res}} = t_{\text{hit}} - t_{\text{event}} - d/c_{\text{ice}}$, at a distance, d , from the emitter:

$$p(t_{\text{res}}, d) = \frac{\tau^{d/\lambda} t_{\text{res}}^{(d/\lambda-1)} e^{t_{\text{res}} + c_{\text{ice}} t_{\text{res}}/X_0 + d/X_0}}{\Gamma(d/\lambda)} \quad (1)$$

Here t_{hit} is the observed time, t_{event} is the time when the photon was emitted. The delay, t_{res} , is not zero because light scatters, mainly due to the presence of small amounts of dust in the ice. The parameters τ , λ and X_0 are obtained from a fit to Monte Carlo. The parameter τ is interpreted as a scattering time, λ as a scattering length and X_0 as an absorption length.

A likelihood function can be constructed in the following way:

$$\mathcal{L} = \prod_{i=0}^{\text{hits}} p(t_{\text{res}}^i, d_i), \quad L = -\log\left(\frac{\mathcal{L}}{N_{\text{ch}} - N_{\text{fit}}}\right), \quad (2)$$

here N_{ch} is the number of hit optical modules and N_{fit} is the number of free parameters of the fit. The product is calculated using all hit optical modules. The maximization of \mathcal{L} provides the most likely position and time of the cascade. The procedure is actually slightly more complicated because the effects of the PMT and electronics jitter have to be taken into account. This problem is solved in the same way it is done for the muon reconstruction (Wiebusch, 1998).

4.2 Energy and Direction Reconstruction: Probability of Hit and No Hit

The probability of a given optical module of observing a signal or not observing a signal is:

$$P_{\text{Hit}} = 1 - e^{-\eta}, \quad P_{\text{NoHit}} = e^{-\eta}, \quad (3)$$

where η is the expected number of photoelectrons. Obviously η is a function of distance from the source to the optical module, the total cascade light output, angular distribution of the light output, etc.

For cascades the total light output is linear with the energy of the cascade (Wiebusch, 1995), and thus $\eta \propto E$. The angle and distance dependences are not trivially derivable from first principles and therefore it has been parametrized as a function of the angle formed between the cascade direction and the vector that joins the cascade vertex to the optical module.

Knowing the functional form of η allows the construction of the likelihood function:

$$\mathcal{L} = \prod_{\text{hit OMs}} P_{\text{Hit}} \prod_{\text{no hit OMs}} P_{\text{NoHit}} \quad (4)$$

Maximization of \mathcal{L} provides the most likely value of energy and direction of the cascade. Note that in principle this procedure also allows for the reconstruction of position (but

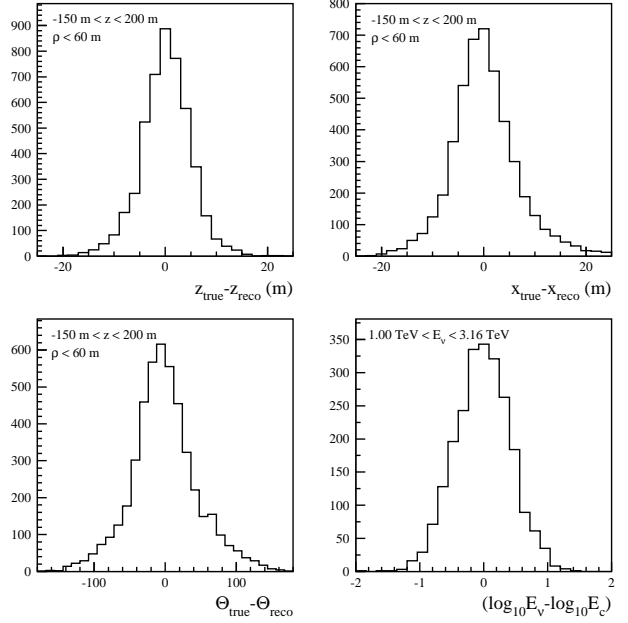


Fig. 1. The upper plots show the difference between true position and reconstructed position for neutrinos that interact inside the detector. The lower left plot shows the difference between the true zenith angle and the reconstructed zenith angle for neutrinos that interact inside the detector. The lower right plot shows the difference between true $\log_{10} E_{\nu}$ and the reconstructed $\log_{10} E_c$. Energy resolution for cascades that interact inside the detector is slightly better. For all the plots, the sample used is $E^{-2} \nu_e$ Monte Carlo processed to cut 3 from table 1.

not time) of the cascade. It has been found, though, that the position resolution obtained with the probability of hit and no hit method, is not as good as with the time delay procedure. The method of probability of hit and no hit has been tuned to measure the energy of an electromagnetic cascade. Hadronic cascades light yield is approximately 80% that of electromagnetic cascades (Wiebusch, 1995). Thus the energy of hadronic cascades will be underestimated by the reconstruction by roughly 20%.

4.3 Reconstruction Performance

To study the performance of the reconstruction algorithms we use the $\nu_e + \bar{\nu}_e$ Monte Carlo with E^{-2} spectrum. The cascades induced by neutrinos are reconstructed and selected using the procedure described in section 5 up to cut 3 (see table 1).

Figure 1 shows distributions of position, zenith and energy resolution for $\nu_e + \bar{\nu}_e$ with E^{-2} spectrum.

The average reconstructed position is no more than 0.6 m away from the true position for all 3 spatial coordinates. For the x and y coordinates the r.m.s. of the distribution is 17.8 m while for the z coordinate it is 7.1 m. If we impose the restriction that the neutrinos interact no farther than 60 m from the axis of the detector ($\sqrt{x_{\text{true}}^2 + y_{\text{true}}^2} < 60$ m), then the r.m.s. of the distributions are 6.4 m for the x and y coordi-

	Cut	Data	Bckg MC
	Filter	5.0×10^6	4.5×10^6
1	$L_c/L_\mu > 1$	2.5×10^6	2.7×10^6
2	$L_c < 7.2$	1.2×10^6	1.9×10^6
3	$N_{\text{unscatt}} \geq 12$	5.9×10^5	1.0×10^6
4	$\theta_\mu > 80^\circ$	1.1×10^5	2.3×10^5
5	$-40^\circ < \theta_c - \theta_{\text{line}} < 20^\circ$	7.4×10^4	4.7×10^4
6	Slices in z_c	2.3×10^4	1.2×10^4
7	$\cos(\theta_c) < -0.6$	134	78
8	$E_c \geq 4 \text{ TeV}$	0	9
9	$\log_{10} E_c - \rho_c/20 - 0.6 \geq 0$	0	0.6

Table 1. Cuts used for search for high energy ν -induced cascades with AMANDA-B10. The number of events left on the experimental data and the background (atmospheric μ and ν) Monte Carlo after each cut is also shown. The background Monte Carlo has been rescaled to match the experimental livetime. The atmospheric muon Monte Carlo has a livetime equivalent to about 10 days.

nates and 5.3 m for the z coordinate.

The reconstructed position is biased to be shifted in the direction of the cascade. The mean of this distribution is 9.7 m and the r.m.s. is 16.7 m. For neutrinos that interact no farther than 60 m from the axis of the detector, the mean of the distribution is 4.2 m and the r.m.s. is 6.2 m.

Resolution on the zenith angle is 26° and it is independent of energy.

The energy reconstruction has a resolution of about 40% in $\log_{10} E_\nu$ in the range 1 TeV - 3 TeV and about 45% in the range 3 TeV - 10 TeV. Energy resolution is slightly better for neutrinos that interact inside the detector.

5 Analysis Technique

The methods described in section 4 cannot be applied to the complete data sample due to CPU limitations. Therefore a fast filter is applied first. The filter consists of cuts on a simple energy estimator, topological characteristics of the event and a simplified muon reconstruction that uses the time flow of the event. These procedures are explained elsewhere (Kowalski, 1999). After the filter the data sample is reduced to about 5×10^6 events.

After the filter, the data are reconstructed using both a cascade hypothesis and a muon hypothesis. For the cascade hypothesis the procedure explained in section 4.1 provides position and time and the procedure explained in section 4.2 provides energy and directional (zenith and azimuth). For the muon hypothesis, reconstruction is done for position, time and direction (zenith and azimuth) (Wiebusch, 1998).

Several quality parameters are used to reduce the data size while maintaining a high efficiency for cascade-like events. These parameters include: The number of hits that arrive almost unscattered from the light source to the optical module, N_{unscatt} (in this analysis a photon is deemed unscattered if the time delay, t_{res} , is between -15 ns and 75 ns), the likelihood parameter of the cascade hypothesis (position-

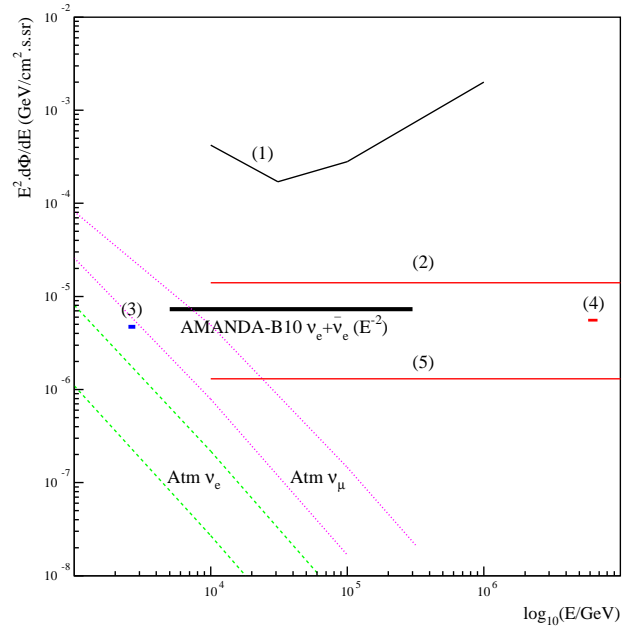


Fig. 2. Spectrum of catastrophic energy losses from atmospheric muons after cut 3 from table 1. The experimental data and Monte Carlo shown correspond to 28 hours live-time.

time), L_c , the ratio of the cascade (position-time) and the muon likelihood parameters, L_c/L_μ , the zenith angle as reconstructed by the cascade hypothesis, θ_c , the zenith angle as reconstructed by the muon hypothesis, θ_μ , the zenith angle as reconstructed by the simplified muon reconstruction, θ_{line} , performed in the filter, the z-component of the position as reconstructed with the cascade hypothesis, z_c , the distance from the reconstructed position to the axis of the detector, $\rho_c = \sqrt{x_c^2 + y_c^2}$ and the reconstructed energy, E_c .

The cut parameters are able to select cascade events that are reconstructed with high quality, because they reduce the background from down going atmospheric muons and because they reduce the background of stochastic energy losses by atmospheric muons.

It has been found that unsimulated instrumental effects, such as crosstalk, produce significant discrepancies between data and atmospheric muon Monte Carlo in certain regions of the detector. Therefore a cut is made to remove slices of the z component of the reconstructed cascade position, z_c .

Table 1 lists the cut parameters and the data passing rates.

6 Sensitivity to High Energy Cascades

It is possible to use energy losses from atmospheric μ to test the energy reconstruction algorithms. After carrying the analysis explained on section 5 up to cut 3 (table 1), the remaining data are dominated by muons with a single large catastrophic energy loss producing most of the hit optical modules in the detector. Figure 2 shows the energy spectra of muon energy losses for experimental data and atmospheric muon Monte Carlo after cut 3.

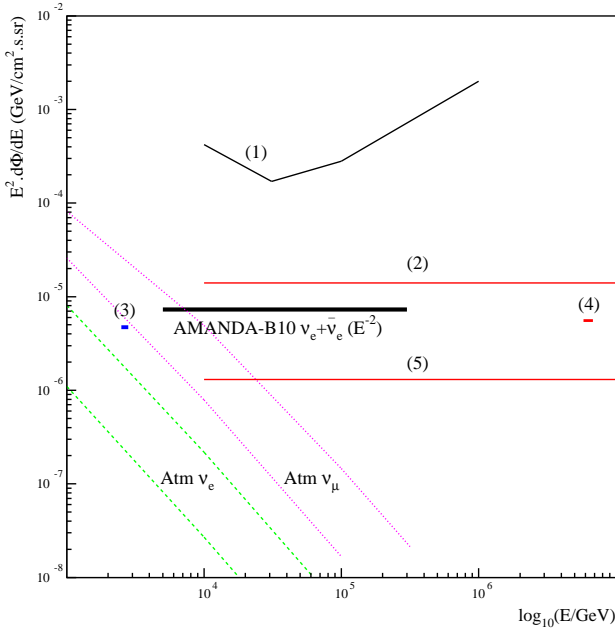


Fig. 3. Various upper limits on the flux of high energy neutrinos. AMANDA-A on $\nu_e + \bar{\nu}_e$ (1) (Porrata *et al.*, 1997); BAIKAL on $\nu_e + \nu_\mu + \bar{\nu}_\mu$ assuming E^{-2} spectrum (2) (Balkanov *et al.*, 2000); Frejus on $\nu_\mu + \bar{\nu}_\mu$ at 2.6 TeV (3) (Rhode *et al.*, 1996); BAIKAL on $\bar{\nu}_e$ (4) at the W resonance (Dzhilkibaev *et al.*, 2001) (4); BAIKAL on $\nu_e + \nu_\mu + \bar{\nu}_\mu$ assuming E^{-2} spectrum (Dzhilkibaev *et al.*, 2001) (5) and AMANDA-B10 on $\nu_e + \bar{\nu}_e$ assuming E^{-2} spectrum (this work). Also shown are the fluxes of atmospheric $\nu_\mu + \bar{\nu}_\mu$ (upper dotted line: horizontal flux, lower dotted line: vertical flux) and atmospheric $\nu_e + \bar{\nu}_e$ (upper dashed line: horizontal flux, lower dashed line: vertical flux) (Lipari, 1993).

The atmospheric μ Monte Carlo under-predicts the energy observed by approximately 0.1 in $\log_{10}(E_c/\text{GeV})$. We can use this shift as an estimation of the systematic error in energy reconstruction. Changing cut 8 by 0.1 in $\log_{10}(E_c/\text{GeV})$ changes the limit by approximately 5%.

Lasers deployed in the ice have been used to study the detector response to cascades with energies in the range 2-200 TeV. It has been found that unsimulated detector effects worsen the limit by no more than 5%.

7 Results

The analysis was applied to Monte Carlo samples of atmospheric neutrinos, $\nu_e + \bar{\nu}_e$ following E^{-2} spectrum, atmospheric muons and to the 1997 data. In the data no events are found. The atmospheric ν Monte Carlo predicts approximately 0.6 events. No events are found in the atmospheric muon Monte Carlo after all cuts. Thus a limit on the flux of $\nu_e + \bar{\nu}_e$, assuming E^{-2} spectrum as typical for Fermi acceleration, can be set via the formula:

$$E^2 \frac{d\phi}{dE} = \frac{N_{90\%}}{TN_A \rho_{\text{ice}} \int E^{-2} \sigma_{\text{total}} V_{\text{eff}} d\Omega dE} \quad (5)$$

Here T is the live-time, N_A is Avogadro's number, ρ_{ice} is ice's density, σ_{total} (Gandhi *et al.*, 1998) is the cross section

for $\nu_e + \bar{\nu}_e$ and V_{eff} is the effective volume of the detector as a function of neutrino energy.

Assuming E^{-2} spectrum, the preliminary 90% C.L. on diffuse flux of $\nu_e + \bar{\nu}_e$ is:

$$\frac{d\phi}{dE} E^2 < 7.3 \times 10^{-6} \frac{\text{GeV}}{\text{s} \cdot \text{cm}^2 \cdot \text{sr}}, \quad (6)$$

where $N_{90\%} = 2.44$ has been determined using the unified Feldman-Cousins procedure (Feldman and Cousins, 1998).

Different available limits on the flux of diffuse neutrinos are shown in figure 3.

8 Conclusions

A search for high energy ν -induced cascades has been conducted with the AMANDA detector using the 1997 data sample. No evidence has been found for the existence of diffuse extraterrestrial electron neutrinos and a limit has been set on their flux. Preliminary studies of detector sensitivity have been performed. A detailed study of systematic errors is in progress and it is not expected to significantly degrade the limit.

The analysis of 1998 and 1999 data, currently ongoing, will increase the live-time by roughly a factor of three.

In the austral summer of 2000, the AMANDA-II upgrade was completed (Wischnewski *et al.*, 2001). This new configuration of AMANDA has an instrumented volume 3 times that of AMANDA-B10 (1997 configuration). We expect that AMANDA-II will have a much improved rejection capabilities of down-going atmospheric muons and thus might be able to separate atmospheric neutrino induced cascades from the background (Wischnewski *et al.*, 2001). Accordingly the sensitivity to cascades induced by extraterrestrial neutrinos should improve significantly.

References

- Andrés E. *et al.* Nature **410** (2001), 441
- Balkanov V.A. *et al.* Astropart. Phys. **14** (2000), 61
- Feldman G. and Cousins R. Phys.Rev.D **57** (1998) 3873
- Dzhilkibaev J. *et al.* Proc. 9th Int. Conf on Neutrino Telescopes, Venice, (2001). astro-ph/0105269
- Hill G. *et al.* Proc 26th ICRC (Salt Lake City) HE.6.3.02 (1999)
- Gandhi R. *et al.* Phys.Rev.D **58** (1999), 093009
- Kowalski, M. Diploma Thesis. *On the Reconstruction of Cascade Like Events in the AMANDA Detector*. Humboldt University (1999)
- Lipari P. Astropart. Phys. **1** (1993), 193
- Porrata R. *et al.* Proc 25th ICRC (Durban) HE.4.1.4 (1997)
- Rhode W. *et al.* Astropart. Phys. **4** (1994), 217
- Stanev T. Phys.Rev.Lett. **83** (1999), 5427
- Wiebusch C. Proc. Workshop: Simulation and Analysis Methods for Large Neutrino Detectors, DESY-Zeuthen, Germany (1998). DESY-PROC-1999-01
- Wiebusch C. PhD Thesis. *The Detection of Faint Light in Deep Underwater Neutrino Telescopes*. RWTH (1995)
- Wischnewski R. *et al.* These proceedings